

## Simultaneous dual-excitation ratiometry using orthogonal linear polarized lights

Takashi Fukano, Satoshi Shimozone, and Atsushi Miyawaki\*

*Laboratory for Cell Function and Dynamics, Advanced Technology Development Group, Brain Science Institute, RIKEN (The Institute of Physical and Chemical Research), 2-1 Hirosawa, Wako-shi, Saitama-ken 351-0198, Japan*

Received 21 January 2004

### Abstract

Dual-excitation ratiometric dyes permit quantitative  $\text{Ca}^{2+}$  measurements by minimizing the effects of several artifacts that are unrelated to changes in the concentration of free  $\text{Ca}^{2+}$  ( $[\text{Ca}^{2+}]$ ). These dyes are excited alternately at two different wavelengths, and the pair of intensity measurements must be collected sequentially. Therefore, it is difficult to follow very fast  $\text{Ca}^{2+}$  dynamics or  $\text{Ca}^{2+}$  changes in highly motile cell samples. Here, we present a novel but simple dual-excitation ratiometric method which overcomes this problem. By the use of our home-made illuminator, each sample is illuminated by two orthogonal linear polarized lights of different wavelengths. Fluorescence images are captured by two CCD cameras through two analyzers, whose polarization directions are at right angles. This methodology allows us to perform simultaneous measurements of any dual-excitation ratiometric dye, and we demonstrate its validity by monitoring  $[\text{Ca}^{2+}]$  changes in rat cardiac muscle cells loaded with Fura Red.

© 2004 Elsevier Inc. All rights reserved.

**Keywords:** Fluorescence imaging; Cardiac cells; Calcium imaging

For quantitative measurements of  $[\text{Ca}^{2+}]$ , ratiometric dyes are preferable [1], because the use of such dyes allows for correction of uneven loading or partitioning of dye within the cell as well as variations in cell thickness. Dual-emission ratiometry provides an ideal readout for fast and confocal microscopy [2]. By contrast, dual-excitation ratiometry has one main disadvantage. Alteration of excitation light between two different wavelengths necessitates a time lag between the two images from which the ratio image is created. The time lag is the composite of the exposure time for the first image and the transition time required to alter the excitation wavelength. The latter is  $>50$  ms for a mechanical filter wheel, or about 1 ms for a monochromator-based wavelength-exchange system composed of a rotating diffraction grating attached to a galvanometer scanner. Although dual-excitation ratiometric dyes for  $[\text{Ca}^{2+}]$ , such as Fura-2, BTC, and ratiometric-pericam [3], are widely used for a variety of applications, it has been difficult to apply them to studies for monitoring

very fast  $\text{Ca}^{2+}$  dynamics or  $\text{Ca}^{2+}$  changes in highly motile cell samples.

To obtain confocal images of  $\text{Ca}^{2+}$  using ratiometric-pericam, we established a compromised system in which two laser beams (excitation: 408 and 488 nm) are alternated on every scanning line under the control of two acousto-optic tunable filters (AOTFs) [4]. This system increases the rate at which ratio measurements are done to 200 Hz and provides confocal images at 1–10 Hz depending on the image size.

Aiming at simultaneous dual-excitation ratiometry, in this study, we employed fluorescence polarization. Fluorescence polarization measurements provide information on the rotational diffusion and orientation distributions of proteins [5]. Viscosity within subcellular organelles and protein behavior (oligomerization, clustering, and complex formation) have been examined by steady-state fluorescence anisotropy techniques. Here, we used this technique to monitor  $\text{Ca}^{2+}$  signaling in cardiac cells, performing dual-excitation ratiometric imaging using a novel optical system that allows simultaneous illumination and detection at any given two wavelengths. This system utilizes two orthogonal linear

\* Corresponding author. Fax: +81-48-467-5924.

E-mail address: [matsushi@brain.riken.go.jp](mailto:matsushi@brain.riken.go.jp) (A. Miyawaki).

polarized lights of different wavelengths, and can detect separately two differently polarized emitted signals of the same wavelength using two cameras.

## Theory

The principle of simultaneous dual-excitation ratiometry with orthogonal linear polarized lights is illustrated in Fig. 1. The explanation will use the fluorescence microscope transmission mode for simplicity and a sample loaded with Fura Red. The extension to other dual-excitable indicators is straightforward. Fura Red is a visible dual-excitable ratiometric  $\text{Ca}^{2+}$  indicator, which has peaks at 472 nm (low  $[\text{Ca}^{2+}]$ ) and 436 nm (high  $[\text{Ca}^{2+}]$ ) in absorption with an isosbestic wavelength of  $\sim 458$  nm [1,6]. Typically, such a sample would be excited alternately at 400 and 490 nm in accordance with the experimental conditions.

First, we suppose that the sample is excited only with light of wavelength 400 nm that is polarized in the plane of the page. The fluorescence emission originating from the sample is depolarized. As a result, it may be detected not only in the original plane, but also in the plane perpendicular to that of excitation light. One main reason for this depolarization is the random orientation of fluorophores; in an actual experiment the cell would contain many fluorophores with a random distribution. Rotational diffusion of fluorophore, radiative reabsorption, and fluorescence resonance energy transfer are

other causes of depolarized fluorescence emission [5]. A polarizing beam splitter is used to separate the fluorescence into two components, one polarized parallel to the excitation polarization and the other polarized perpendicular to it. Two CCD cameras (CCD1 and CCD2) capture the two fluorescence images simultaneously. Here, the total emission intensity following 400-nm excitation,  $I_{400}$ , is expressed as:

$$I_{400} = I_{400,\text{CCD1}} + I_{400,\text{CCD2}}, \quad (1)$$

where  $I_{400,\text{CCD1}}$  and  $I_{400,\text{CCD2}}$  are the intensities obtained from CCD1 and CCD2, i.e., the components of fluorescence intensity emitted with polarization parallel and perpendicular, respectively, to the excitation light.

Second, suppose the sample is excited with light of wavelength 490 nm that is polarized perpendicular to the original 400-nm-excitation light. Similarly, the fluorescence intensity,  $I_{490}$ , resulting from this excitation may be denoted as:

$$I_{490} = I_{490,\text{CCD1}} + I_{490,\text{CCD2}}, \quad (2)$$

where  $I_{490,\text{CCD1}}$  and  $I_{490,\text{CCD2}}$  are the intensities obtained from CCD1 and CCD2. Now, when the sample is excited simultaneously with mutually orthogonal linear polarized light of both 400 and 490 nm, the resulting fluorescence images,  $I_{\text{CCD1}}$  and  $I_{\text{CCD2}}$ , captured by CCD1 and CCD2 are expressed as:

$$I_{\text{CCD1}} = I_{400,\text{CCD1}} + I_{490,\text{CCD1}} \quad (3)$$

and

$$I_{\text{CCD2}} = I_{400,\text{CCD2}} + I_{490,\text{CCD2}}. \quad (4)$$

We assume that the ratios between the components of the fluorescence intensities emitted with polarization parallel and perpendicular to the excitation light are constant during experiment:

$$r_{400} = \frac{I_{400,\text{CCD2}}}{I_{400,\text{CCD1}}} = \text{constant}, \quad (5)$$

$$r_{490} = \frac{I_{490,\text{CCD1}}}{I_{490,\text{CCD2}}} = \text{constant}. \quad (6)$$

It is noted that both  $r_{400}$  and  $r_{490}$  range from 0 to 1. Combining Eqs. (1)–(6) yields the following equations:

$$I_{400} = \frac{1 + r_{400}}{1 - r_{400}r_{490}} (I_{\text{CCD1}} - r_{490}I_{\text{CCD2}}), \quad (7)$$

$$I_{490} = \frac{1 + r_{490}}{1 - r_{400}r_{490}} (-r_{400}I_{\text{CCD1}} + I_{\text{CCD2}}). \quad (8)$$

In this way, it is possible to obtain the emission intensity from the 400-nm excitation ( $I_{400}$ ) and the 490-nm excitation ( $I_{490}$ ) independently from two CCD images, which are obtained from simultaneous excitations with orthogonal linear polarization. In addition, the fluorescence ratio image is simply calculated by  $I_{400}/I_{490}$ .

We need to discuss in detail the conditions under which Eqs. (7) and (8) are valid. If the denominator takes 0 or  $r_{400}r_{490} = 1$ , there will be no solution to Eqs.

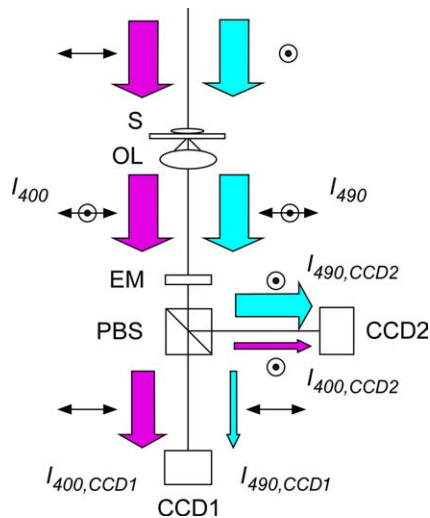


Fig. 1. The principle of simultaneous dual-excitation ratiometry with orthogonal linear polarized light. Fura Red within the sample is excited by light of 400 nm and/or 490 nm. The 400-nm-excitation light is linearly polarized in the plane of the page, whereas the 490-nm light is linearly polarized perpendicular to the page. The polarizing beam splitter transmits light polarized in the plane of the page and reflects light polarized perpendicular to the page. The arrows represent the states of polarization of light. S, sample; OL, objective lens; EM, emission filter; PBS, polarizing beam splitter; and CCD, charge coupled device.

(7) and (8). This will occur when (a)  $r_{400} = 1/r_{490}$  or (b)  $r_{400} = r_{490} = 1$ . However, condition (a) is not possible because both  $r_{400}$  and  $r_{490}$  are defined as having a range from 0 to 1 in Eqs. (5) and (6). Condition (b) is realized when the fluorescence is completely depolarized. In this case, it would not be possible to obtain separate fluorescence images with simultaneous excitation.

The application of our proposed method requires that the following two conditions be satisfied:

- (1) The fluorescence ratio must be constant during the experiment.
- (2) For each excitation wavelength, the fluorescence ratio between the two polarization states must not be equal to 1.

This method is based on the statistical feature of fluorescence polarization and is not applicable to analyzing single fluorescent molecules or fluorescent speckles [7].

## Materials and methods

### Chemical dyes

Fura Red, Fura-2, and BTC were purchased from Molecular Probes. The salt forms of Fura Red, Fura-2, and BTC were diluted with PBS (phosphate-buffered saline) buffer solution to a final concentration of  $\sim 10 \mu\text{M}$ . A  $\sim 200 \mu\text{l}$  droplet of each solution was sandwiched between two coverslips and imaged at  $25^\circ\text{C}$ .

### Fluorescence proteins

Ratiometric-pericam, a dual-excitable  $\text{Ca}^{2+}$  indicator based on yellow fluorescence protein [3], was prepared. Enhanced green fluorescence protein (EGFP) and DsRed2 (Clontech) were expressed in *Escherichia coli* and purified. The recombinant proteins were then diluted with PBS buffer solution to a concentration of  $\sim 0.1 \text{ mg/ml}$ . A  $\sim 200 \mu\text{l}$  droplet of each solution was sandwiched between two coverslips and imaged at  $25^\circ\text{C}$ .

### Cell preparation

**HeLa cells.** HeLa cells were grown on 35-mm glass-bottomed dishes. They were maintained in Dulbecco's modified Eagle's medium supplemented with 10% fetal bovine serum at  $37^\circ\text{C}$  in 5%  $\text{CO}_2$ . Two or three days after cDNA transfection with lipofectin (Gibco/BRL), cells in Hanks' balanced salt solution buffer were imaged at  $25^\circ\text{C}$ .

For loading dye into cells, the acetoxymethyl (AM) ester forms of Fura Red, BTC, and Fura-2 were used. Dye loading was performed according to the manufacturer's instructions; HeLa cells were incubated at  $37^\circ\text{C}$  for 30 min at a final working concentration of 10, 2, and  $10 \mu\text{M}$  for Fura Red, Fura-2, and BTC, respectively. After the dye loading, cells were washed twice with Hanks' balanced salt solution buffer and suspended in the same media. After 10 min, cells were imaged at  $25^\circ\text{C}$ .

**Cardiac muscle cells.** Preparation of cardiac muscle cells was accomplished according to a protocol similar to one previously described [8,9]. The heart was removed and rapidly placed in ice-cold PBS containing 116 mM NaCl, 0.8 mM  $\text{NaH}_2\text{PO}_4$ , 5.3 mM KCl, 0.4 mM  $\text{MgSO}_4$ , 5 mM glucose, and 20 mM Hepes, pH 7.35. Hearts were submitted to four subsequent digestions with 0.125% trypsin. The first supernatant containing cell debris and blood cells was discarded. Cell suspensions from the three subsequent digestions (20 min each) were

centrifuged and the pellets were resuspended in 2 ml DMEM. Cells were pooled and resuspended in a complete DMEM containing penicillin (100 U/ml), streptomycin (100 mg/ml), and 10% FBS. Cells were then incubated for 1 h at  $37^\circ\text{C}$ , allowing the selective attachment of non-myocytes. The unattached cells were plated at a density of  $0.6 \times 10^6$  cell/ml onto 35 mm diameter glass-bottomed dishes. On the first day of culture, cells were washed and maintained in DMEM with 10% FBS. The loading of Fura Red to cardiac muscle cells was carried out by the same procedure as with the HeLa cells.

### Fluorescence polarization measurements

**Optical configuration.** Fig. 2 illustrates the transmission type fluorescence microscope that was used in this study. A 75-W xenon lamp was used as an excitation light source. The light from the lamp was wavelength-filtered by an excitation filter and became linearly polarized light after passing through a polarizer (Shiguma-koki, SPF-30C-32). The sample was excited by the light after passing through an objective lens (OL1, Olympus MDPlan,  $10\times$ , NA 0.25). Another objective (OL2, Olympus UAPO340,  $40\times$ , NA1.35) was used, together with a tube lens, to project the fluorescence image onto a CCD camera (CoolSNAP-HQ, Roper scientific). An analyzer, identical to the polarizer, and an emission filter were inserted into the detection path. The excitation and emission filters used for each indicator are listed in Table 1.

**Experimental procedure and data analysis.** The polarization state of the fluorescence from the sample was examined by rotating the analyzer under excitation with linearly polarized light. Fluorescence images were recorded every  $10^\circ$  of the azimuth angle of the analyzer. The azimuth angle of  $0^\circ$  was adjusted so that the direction of the analyzer was parallel to that of the polarizer. For dual-excitable indicators, we measured the polarization after excitation with wavelengths longer and shorter than the isosbestic wavelength. Exposure time was set to 500–2000 ms.

The data analysis was performed via the following steps. First, the background signal, including auto-fluorescence and dark-current

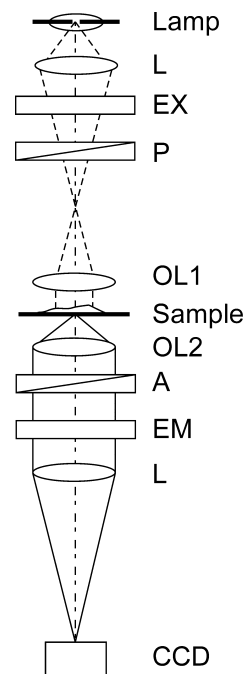


Fig. 2. Schematic diagram of the optical configuration used to measure the fluorescence polarization. L, lens; EX, excitation filter; P, polarizer; OL, objective lens; A, analyzer; EM, emission filter; and CCD, charge coupled device.

Table 1

Measured results of the fluorescence polarization ratio  $r$  and the angular difference between the direction of polarization of the excitation light and the direction of the analyzer at which the maximum fluorescence  $\varphi$  is observed

Indicator	Filter		Solution		Cell	
	EX	EM	$r$	$\varphi$ (deg)	$r$	$\varphi$ (deg)
Fura Red	400DF15	565EFLP	$0.79 \pm 0.002$	$-1.6 \pm 0.42$	$0.66 \pm 0.034$	$-0.3 \pm 6.67$
	490DF20	565EFLP	$0.78 \pm 0.002$	$1.1 \pm 0.17$	$0.63 \pm 0.032$	$-2.1 \pm 6.66$
Fura-2	340HT15	510WB40	$0.83 \pm 0.001$	$0.9 \pm 0.38$	$0.68 \pm 0.017$	$0.3 \pm 0.88$
	380HT15	510WB40	$0.84 \pm 0.001$	$0.7 \pm 0.57$	$0.66 \pm 0.024$	$-0.2 \pm 1.44$
BTC	400DF15	535DF25	$0.89 \pm 0.002$	$0.3 \pm 0.51$	$0.67 \pm 0.033$	$6.5 \pm 1.55$
	490DF20	535DF25	$0.89 \pm 0.002$	$1.2 \pm 0.40$	$0.65 \pm 0.025$	$0.9 \pm 2.00$
Ratiometric-pericam	400DF15	535DF25	$0.71 \pm 0.002$	$0.9 \pm 0.52$	$0.63 \pm 0.050$	$6.1 \pm 3.48$
	490DF20	535DF25	$0.73 \pm 0.002$	$1.0 \pm 0.47$	$0.66 \pm 0.044$	$6.4 \pm 4.46$
EGFP	475AF40	535DF25	$0.76 \pm 0.004$	$1.6 \pm 0.30$	$0.66 \pm 0.041$	$3.7 \pm 2.08$
DsRed2	540AF30	575ALP	$0.82 \pm 0.002$	$2.4 \pm 0.41$	$0.69 \pm 0.008$	$3.2 \pm 1.11$

Excitation and emission filters are also cited. Results are the composite of five individual measurements, expressed as means  $\pm$  SD.

noise, was subtracted for each fluorescence image. Second, the following equation was fitted to the fluorescence data, which were obtained by averaging fluorescence intensity in the appropriate region, with respect to the azimuth angle of the analyzer;

$$I = a + b \cos[2(\theta + \varphi)], \quad (9)$$

where  $I$  is the fluorescence intensity,  $a$  and  $b$  are the bias and amplitude components of the fluorescence intensity, respectively,  $\theta$  is the azimuth angle of the analyzer, and  $\varphi$  is the angular difference between the polarization direction of excitation light and the direction of the analyzer at which the maximum fluorescence was observed. Third, the fluorescence polarization ratio  $r$  between the maximum  $I_{\max}$  and the minimum  $I_{\min}$  of the fluorescence intensity was calculated by

$$r = \frac{I_{\min}}{I_{\max}} = \frac{a - b}{a + b}. \quad (10)$$

For presentation of pseudo-color images, intensity-modulated display mode was adopted. Fluorescence images (12 bits coded for 4096 intensity levels) were superimposed onto 8 bit-pseudo-color ratio images.

#### Simultaneous dual-excitation ratiometry

**Optical configuration.** Fig. 3 shows the optical configuration, which was based on an inverted fluorescence microscope (Olympus, IX71, Tokyo). Arrows represent the states of polarization of light. Light originated from a 75 W xenon arc lamp and was divided into two beams by a polarizing beam splitter (PBS1, 10BC17MB.1, Newport). The beams were then filtered either by a 385–425 nm (EX1, 405DF40, Omega Optical) or a 480–500 nm excitation filter (EX2, BP480-500, Olympus). After passing through polarizers (S342-20-550, Suruga-seiki) which were inserted into the each optical path to ensure the correct linear polarization, the beams were then superimposed by the use of a second polarizing beam splitter (PBS2). Thus, the beams leaving the polarizing beam splitter are coaxial and have mutually orthogonal linear polarization states with different wavelengths. The light was relayed by lenses (L2, L3), reflected by a dichroic mirror (505DRLPXR, Omega Optical), and then projected onto the sample, with the correct polarization states maintained, after passing through an objective lens (UAPO340, 40 $\times$ , NA1.35, Olympus). The fluorescence emitted by the sample was filtered by an emission filter (530ALP, Omega Optical) and divided into two beams by a third polarizing beam splitter (PBS3), and each of these was focused onto a different CCD camera (CoolSNAP-HQ, Roper scientific) after passing through tube lenses (L4, L5). An analyzer was inserted in front of each camera to purify the incoming polarized light (Shiguma-koki, SPF-30S-32).

**Imaging and data analysis.** The images captured by the CCDs were simultaneously transferred to a personal computer. Image acquisition and subsequent image processing were performed by imaging software (MetaMorph 4.6, Universal Imaging, Media, PA). We used the

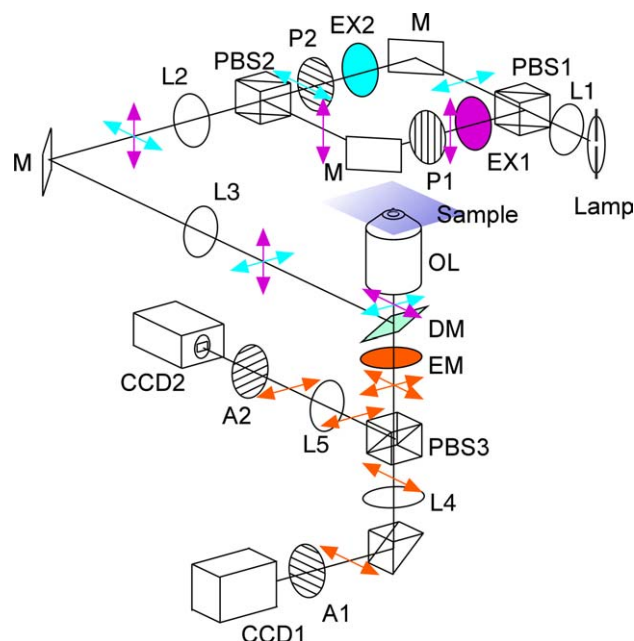


Fig. 3. Schematic diagram of the optical configuration. L, lens; PBS, polarizing beam splitter; M, mirror; EX1 and EX2, excitation filters for 400 and 490 nm light, respectively; P, polarizer; DM, dichroic mirror; OL, objective lens; EM, emission filter; and A, analyzer. The arrows represent the polarization states of the light.

“stream acquisition mode” of MetaMorph, by which the images are captured as rapidly as possible in a continuous data stream and stored in the random access memory of the computer. With the exposure time set at 30 ms, the interval time with the camera binning set at 8 was 70 ms. Each sample was maintained at 37 °C during the experiment. The fluorescent images  $I_{400}$  and  $I_{490}$  excited with 400-nm-excitation and 490-nm-excitation lights were calculated by using Eqs. (7) and (8), respectively, from images  $I_{\text{CCD1}}$  and  $I_{\text{CCD2}}$  captured by cameras CCD1 and CCD2. The fluorescence ratios  $r_{400}$  and  $r_{490}$ , which are needed to calculate the fluorescent images  $I_{400}$  and  $I_{490}$ , were obtained from the same sample after the simultaneous excitation experiment. At first, by blocking the 490-nm excitation, we captured the fluorescence images  $I_{400, \text{CCD1}}$  and  $I_{400, \text{CCD2}}$  with only 400-nm-excitation light. Next, we also captured the fluorescence images  $I_{490, \text{CCD1}}$  and  $I_{490, \text{CCD2}}$  with excitation at 490 nm in the same manner. Time-averaged fluorescent ratios  $r_{400}$  and  $r_{490}$  were calculated by using Eqs. (5) and (6), respectively, on the images obtained.

## Results and discussion

### Fluorescence polarization measurements

Figs. 4A and B show the results from the Fura Red solution alone and from HeLa cells loaded with Fura Red, respectively, whereas Figs. 4C and D show the results from the EGFP solution and from HeLa cells

transfected with EGFP. The calculated ratio  $r$  and angular difference between the polarized excitation light and the angle  $\varphi$  at which the emission intensity reaches a maximum, including the results from other dyes and fluorescent proteins, are summarized in Table 1.

The ratio value of Fura Red was evidently larger when it was in solution than when inside the cell (Figs. 4A and B). A similar tendency was observed for other

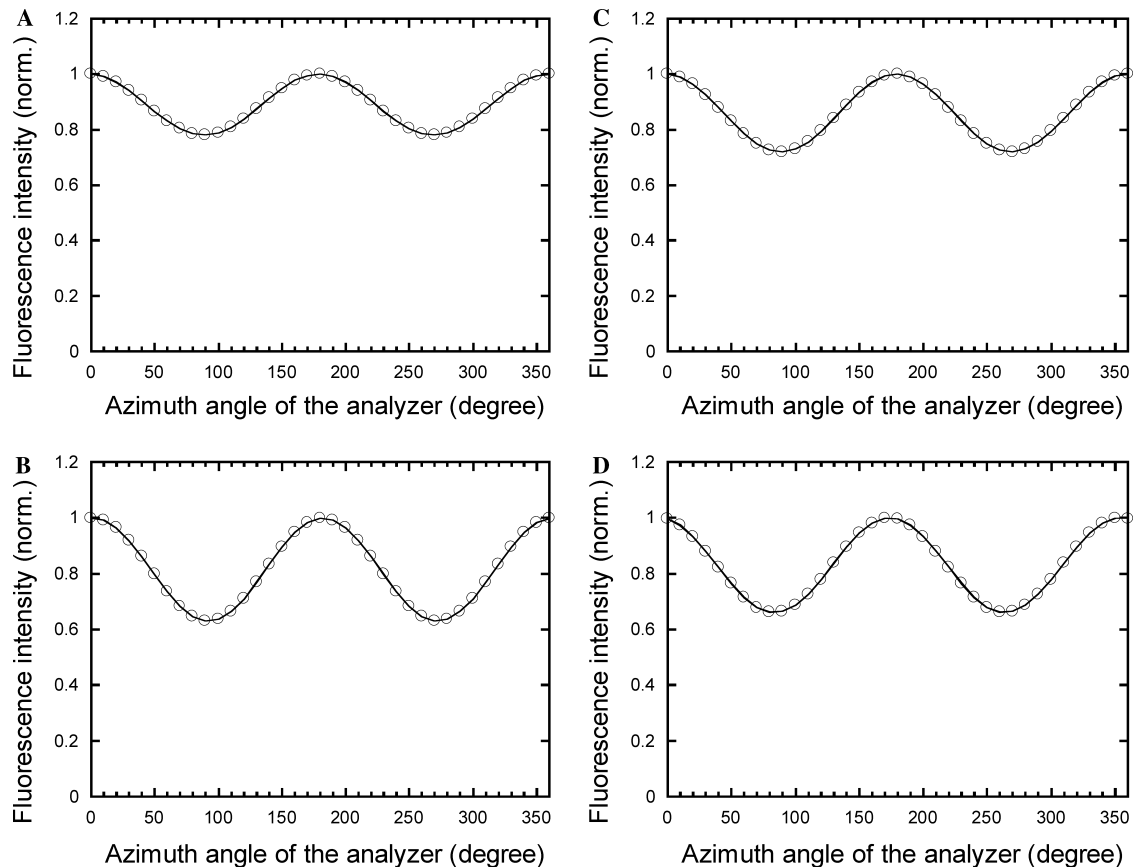


Fig. 4. The results of fluorescence polarization measurements. (A) and (B) are results from Fura Red excited at 490 nm, whereas (C) and (D) are results from EGFP excited at 475 nm. (A) and (C) are obtained from the solution, whereas (B) and (D) are obtained from HeLa cells. Each trace is normalized to the maximum intensity.

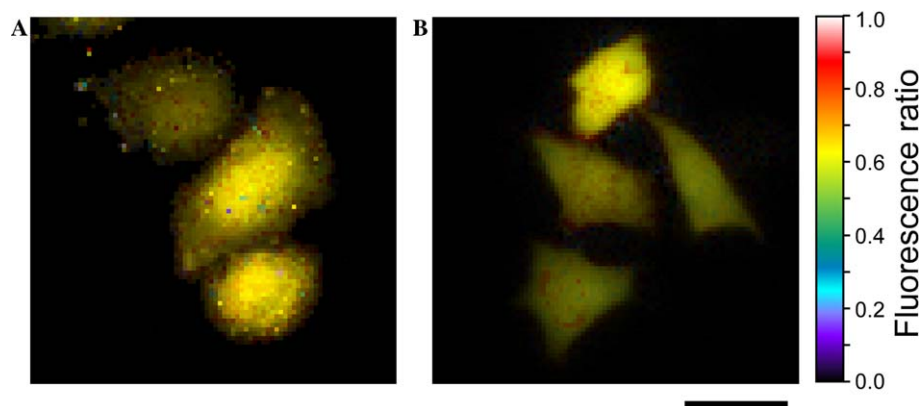


Fig. 5. Maps of  $r$  values for Fura Red (A) and EGFP (B). The images are presented in intensity-modulated display mode, which associates color hue with  $r$  value and the intensity of each hue with the fluorescence image brightness. Scale bar, 20 μm.



indicators. This means that the depolarization caused by the rotational diffusion of the fluorophore is greater when the molecules are free-floating in solution; the rotational diffusion is restricted within the cell because most of the fluorophores bind surrounding proteins.

Also, the fluctuation of the angular difference of the fluorophores was uniformly greater in the cell than when in solution. It is probable that the orientation of the fluorophore dipole is inhomogeneous in the cell, whereas the fluorophore dipoles are all randomly

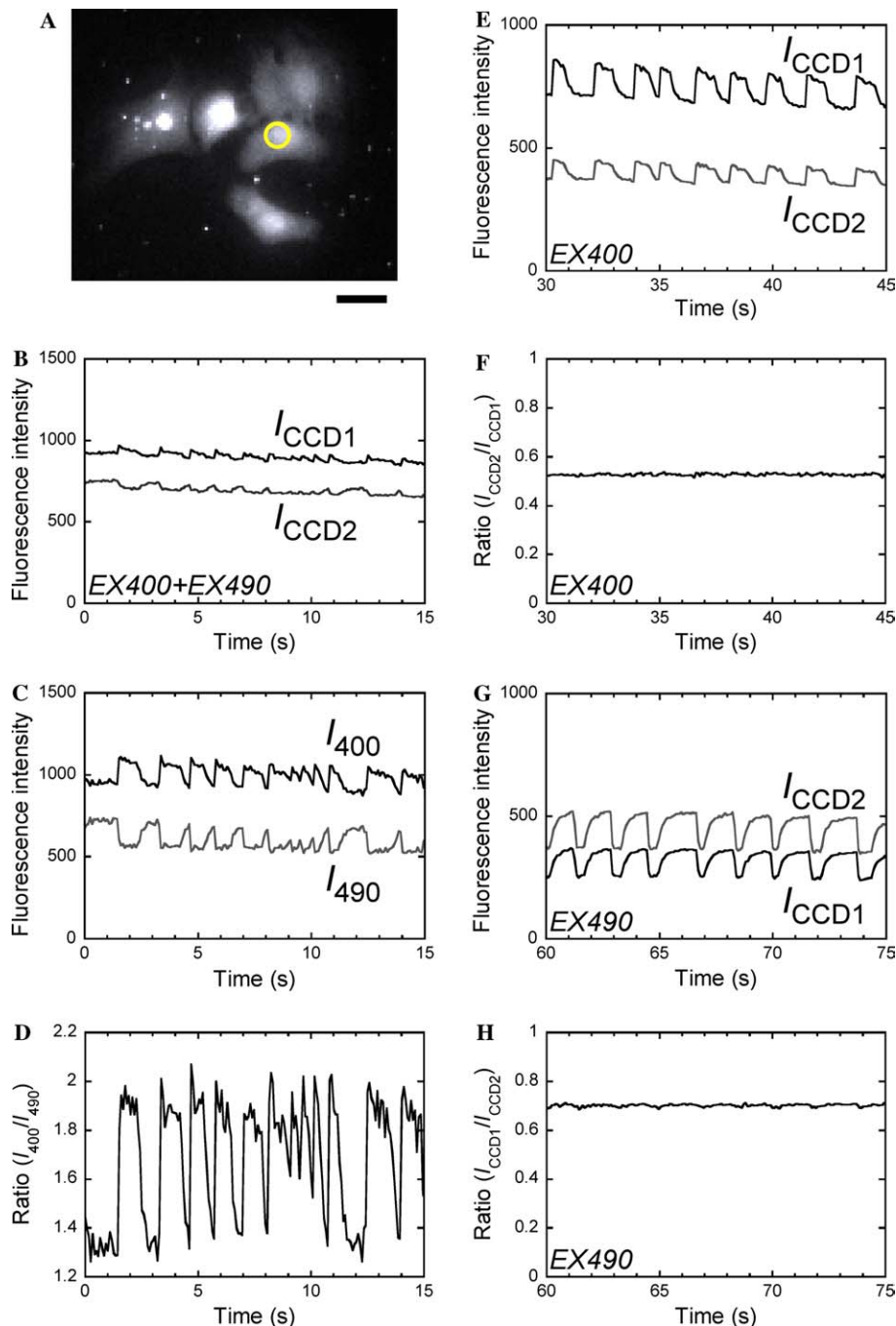


Fig. 6. Ratiometric measurement of  $[Ca^{2+}]$  by simultaneous dual-excitation ratiometry with orthogonal linear polarized lights. (A) Beating cultured cardiac cells loaded with Fura Red were excited at 400 and 490 nm with orthogonal polarization states simultaneously. (B) Raw data of the fluorescence intensities  $I_{CCD1}$  and  $I_{CCD2}$  in a region indicated by a circle in (A). (C) Calculated fluorescence intensities  $I_{400}$  and  $I_{490}$  from data shown in (B), which correspond to the fluorescence intensities obtained by excitation of only 400 nm or only 490 nm, respectively. (D) Fluorescence ratio of the calculated fluorescence intensities  $I_{400}$  and  $I_{490}$ . (E) Raw data of fluorescence intensity profile induced by excitation at 400 nm with both CCDs in the same region of (A). (F) Ratio between CCD1 and CCD2 channels in (E). (G) Fluorescence intensity profile resulting from excitation at 490 nm in the same region of (A). (H) Ratio between CCD1 and CCD2 channels in (G). Scale bar, 20  $\mu m$ .

oriented in solution. On the other hand, the ratio value of the chemical indicators was in general larger than that of the fluorescent proteins. This is because the rotational speed of the fluorescent proteins is lower than that of the chemical indicators, due to differences in the size of the molecules. In all cases where ordinary fluorophores were introduced into cells, the ratio values ranged from 0.6 to 0.7, which satisfied condition (2) of the theory. The ratio values for Fura Red and EGFP were constant over the cells (Figs. 5A and B, respectively).

#### *Simultaneous dual-excitation ratiometry with cardiac muscle cells*

Spontaneously beating cultured cardiac muscle cells loaded with Fura Red were analyzed. The fluorescence image captured by CCD1 is shown in Fig. 6A. Fig. 6B shows the raw data of fluorescence intensity profiles obtained by CCD1 and CCD2 in the region indicated by a circle in Fig. 6A. Then  $I_{400}$  and  $I_{490}$  were calculated from the images of Fig. 6B using Eqs. (7) and (8) (Fig. 6C). In the calculation,  $r_{400} = 0.54$ ,  $r_{490} = 0.70$  were used, both of which were derived from a follow-up experiment.  $I_{400}$  and  $I_{490}$  changed reciprocally throughout the time course, as would be expected. Fig. 6D shows the ratio of  $I_{400}$  to  $I_{490}$ , which reported reliable changes in  $[Ca^{2+}]$  during cardiac contraction. Particularly, the artifact caused by lateral shift of contracting cells, which is often experienced in ordinary dual-excitation ratiometry, was fully eliminated.

After the simultaneous dual-excitation experiment, the same sample was excited by each of the wavelengths in turn. Fig. 6E shows the fluorescence intensity profiles resulting from 400-nm excitation, i.e.,  $I_{400,CCD1}$  and  $I_{400,CCD2}$ , in the region indicated in Fig. 6A. Their ratio value  $r_{400}$  proved to be constant (0.54) during the experiment (Fig. 6F). Subsequently, fluorescence intensities ( $I_{490,CCD1}$  and  $I_{490,CCD2}$ ) were also recorded in the same region following excitation at 490 nm (Fig. 6G). The ratio value  $r_{490}$  was also constant (0.70) (Fig. 6H). The constancy of both  $r_{400}$  and  $r_{490}$  met condition (1) of the theory. The discrepancy between  $r_{400}$  and  $r_{490}$  can be explained by the difference in sensitivity of the two CCDs and the difference in transmittance of the optical components, though these factors should not affect the simultaneous dual-excitation ratiometry. When the traces in Fig. 6C are compared with those in Fig. 6E or Fig. 6G, the waveforms of  $I_{400}$  and  $I_{490}$  were remarkably similar to what were actually observed when the sample was excited by each of the wavelengths in turn, implying the validity of the proposed method.

## Conclusion

We have proposed a new method for simultaneous measurement of dual-excitable ratiometric indicators. This method allows us to capture two separate fluorescence images with different excitation wavelengths without any time lag. We demonstrate its validity by monitoring changes in  $Ca^{2+}$  concentrations in rat cardiac muscle cells loaded with Fura Red, but the proposed method will be successfully applied to any other dual-excitable indicator and a wide variety of applications.

## Acknowledgments

The authors thank H. Mizuno for useful suggestions. We would also like to acknowledge the technical support of Y. Aono (Olympus). This research was partly supported by grants from Core Research for Evolutional Science and Technology (Japan Science and Technology Corporation) and by the Special Coordination fund for the promotion of the Ministry of Education, Culture, Sports, Science and Technology of Japan.

## References

- [1] A.W.M. Simpson, Fluorescence Measurement of  $[Ca^{2+}]_c$ , in: D.G. Lambert (Ed.), *Methods in Molecular Biology, Calcium Signaling Protocols*, Vol. 114, Humana Press Inc., Totowa, New Jersey, 1999, pp. 3–30.
- [2] T. Kawanishi, H. Asou, T. Kato, C. Uneyama, K. Toyoda, H. Ohata, K. Momose, M. Takahashi, Ratio-imaging of calcium waves in cultured hepatocytes using rapid scanning confocal microscope and indo-1, *Bioimages* 2 (1994) 7–14.
- [3] T. Nagai, A. Sawano, E.S. Park, A. Miyawaki, Circularly permuted green fluorescent proteins engineered to sense  $Ca^{2+}$ , *Proc. Natl. Acad. Sci. USA* 98 (2001) 3197–3202.
- [4] S. Shimozono, T. Fukano, T. Nagai, Y. Kirino, H. Mizuno, A. Miyawaki, Confocal imaging of subcellular  $Ca^{2+}$  concentrations using a dual-excitation ratiometric indicator based on green fluorescent protein, *Sci. STKE* 2002 (2002) p14.
- [5] J.R. Lakowicz, *Principles of Fluorescence Spectroscopy*, second ed., Kluwer Academic/Plenum Publishers, New York, 1999.
- [6] N. Kurebayashi, A.B. Harkins, S.M. Baylor, Use of Fura Red as an intracellular calcium indicator in frog skeletal muscle fibers, *Biophys. J.* 64 (1993) 1934–1960.
- [7] C.M. Waterman-Storer, E.D. Salmon, Fluorescent speckle microscopy of microtubules: how low can you go?, *FASEB J.* 13 (1999) S225–S230.
- [8] D.E. Dostal, K.N. Rothblum, K.M. Conrad, G.R. Cooper, K.M. Baker, Detection of angiotensin I and II in cultured rat cardiac myocytes and fibroblasts, *Am. J. Physiol.* 263 (1992) C851–C863.
- [9] V. Robert, P. Gurlini, V. Tosello, T. Nagai, A. Miyawaki, F.D. Lisa, T. Pozzan, Beat-to-beat oscillations of mitochondrial  $[Ca^{2+}]$  in cardiac cells, *EMBO J.* 20 (2001) 4998–5007.